

A dynamic model of transient NH_4^+ assimilation in red algae

Juan J. Vergara^{1,*} F. X. Niell², Kimon T. Bird^{3,**}

¹Departamento de Ecología, Facultad de Ciencias del Mar, Universidad de Cádiz, Apdo. 40,
E-11510 Puerto Real, Cádiz, Spain

²Departamento de Ecología, Facultad de Ciencias, Universidad de Málaga, Campus de Teatinos, E-29071 Málaga, Spain

³Center for Marine Science Research, University of North Carolina at Wilmington, 7205 Wrightsville Av., Wilmington,
North Carolina 28043, USA

ABSTRACT: A dynamic model has been developed describing the effects of transient N assimilation following NH_4^+ pulses on protein synthesis and on C mobilization in red algae. The model simulations indicate that the differential response of phycobiliproteins to N availability seems to be related to a more general response of chloroplast proteins to N supply. The model displays a high robustness. The incorporation of different functions of amino acid transport between the chloroplast and cytosol fractions, as well as different initial distributions of amino acids between these fractions, has little effect on N incorporation at the protein level, with chloroplast proteins being much more affected than cytosolic ones by the variation of the external forcing function, the NH_4^+ supply. With respect to cell C metabolism, the main changes promoted by a transient NH_4^+ assimilation were not in total cell C but in the allocation of C between C reserve structures (carbohydrates) and organic N compounds (amino acids and proteins). The stoichiometry of 6 C molecules needed per N molecule assimilated seems to be crucial in determining the rate of C mobilization in response to transient N assimilation. The development of the model provides further insights in the mechanism of C-N interaction in marine red algae, where the presence of particular N compounds such as phycobiliproteins and of C compounds such as cell wall polysaccharides and floridean starch is different compared to green algae and higher plants. The results of the simulations compared favorably with the experimental data reported for the red alga *Gracilariopsis lemaneiformis*.

KEY WORDS: Ammonia · Carbohydrates · Modelling · Nitrogen assimilation · Phycobiliproteins · Rhodophyta

INTRODUCTION

In ecology there is an extensive tradition in modelling aquatic ecosystems, particularly phytoplankton growth in terms of mass and energy fluxes (see, for instance, Kremer & Nixon 1978, Wiegert 1979, Kiefer & Mitchell 1983, Falkowski et al. 1985, Wulff et al. 1989, Laws & Chalup 1990, Geider et al. 1996). Physiological models have also been coupled to ecological questions to develop new approaches to understanding various acclimation responses (Mooney 1991). In a previous

study (Vergara et al. 1995), we raised 2 questions to be addressed with respect to the response of red alga *Gracilariopsis lemaneiformis* following transient NH_4^+ pulses. First, is the sensitivity of phycobiliproteins to N availability somehow related to a more general response of chloroplast proteins to N supply? Second, what is the stoichiometry of C mobilization in response to transient NH_4^+ assimilation? The model presented here is intended to clarify these questions, imposing a number of theoretical constraints to be checked. We have analyzed the compartmentalization of protein synthesis between chloroplast and cytosol, assaying different kinds of amino acid (aa) transport across the chloroplast membranes, and the stoichiometry of C requirement to support N assimilation into organic N

*E-mail: juanjose.vergara@uca.es

**Kimon Bird died suddenly and unexpectedly at the end of October 1996. He will be sorely missed

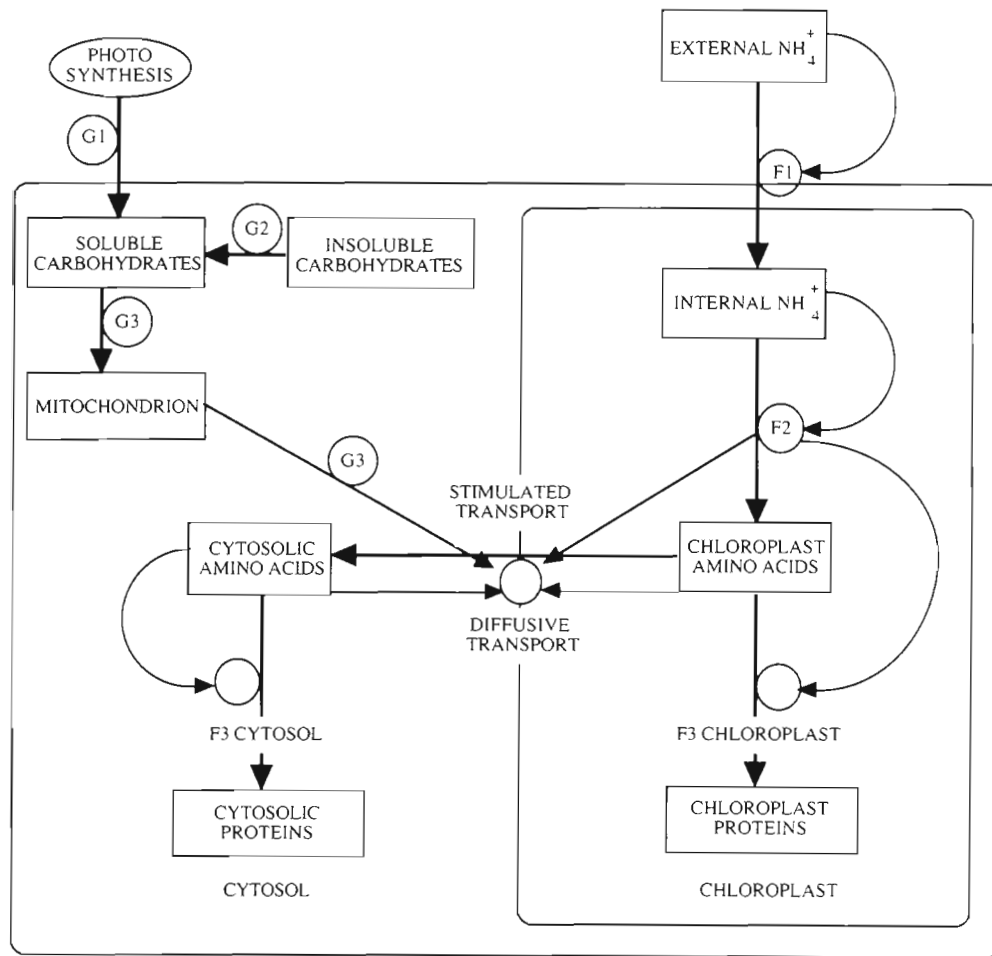


Fig. 1. Diagrammatic representation of the model showing the simulated subcellular compartmentalization of cell C and N variables and flows. State variables (boxes) are joined by arrows that indicate the mass flow of C and N at the cellular level. Circles represent the functions regulating the flows among the compartments

compounds (amino acids and proteins). The simulation of the model indicates that both processes, differential protein synthesis in chloroplasts, and close stoichiometry between C and N assimilation, are key elements in determining the control of C and N allocation in red algae.

FORMULATION OF THE MODEL

The model is made up of a transference matrix (where the nodules α_{ij} express the relationships among the variables) and a state vector, which represents the state of the variables at a given time. These rates (α_{ij}) are not constants, but functions of the instantaneous concentration of the different variables involved through several equations. To facilitate the simulation, differential equations have been transformed to difference equations by means of a numerical integration (Euler's method, Jeffries 1988):

$$\frac{dx}{dt} = \sum_{i=1}^n f_i \rightarrow X_{t+\Delta t} = X_t + \Delta t(f_1 + f_2 + \dots + f_n) \quad (1)$$

The model was run over a period of 6 h, with a Δt of 0.01 h. The relationships among the variables involved in transient N assimilation are shown in Fig. 1. A notation list is provided (Table 1). Dry weight is denoted as DW.

Difference equations of N metabolism. In response to an initial pulse of NH_4^+ , external NH_4^+ concentration will decrease in accordance with the uptake rate of NH_4^+ (F_1):

$$\frac{d[\text{NH}_4^+ \text{Ext.}]}{dt} = -F_1 \quad (2)$$

The variation of the concentration of internal NH_4^+ is a net balance between the net entrance of external NH_4^+ (F_1) and the net rate of aa synthesis (F_2):

$$\frac{d[\text{NH}_4^+ \text{Int.}]}{dt} = F_1 - F_2 \quad (3)$$

This assumes that the production of NH_4^+ via the nitrate and nitrite reductase pathway will be insignificant in comparison with the uptake of external NH_4^+ , as discussed previously (Vergara et al. 1995).

The variation of the concentration of aa is a net balance between the net rate of aa synthesis (F_2) and the

net rate of protein synthesis (F_3):

$$\frac{d[aa]}{dt} = F_2 - F_3 \quad (4)$$

The variation of the concentration of proteins ($prot$) will depend on its rate of synthesis (F_3):

$$\frac{d[prot]}{dt} = F_3 \quad (5)$$

Table 1. Symbols and units of the state variables, flows and parameters of the model. DW: dry weight

State variables	
$NH_4^+ Ext.$	External ammonia concentration ($\mu\text{mol } NH_4^+ \text{ g}^{-1} \text{ DW}$)
$NH_4^+ Int.$	Internal ammonia concentration ($\mu\text{mol } NH_4^+ \text{ g}^{-1} \text{ DW}$)
aa	Amino acid concentration ($\mu\text{mol } aa \text{ g}^{-1} \text{ DW}$)
aa_{chlor}	Chloroplast amino acid concentration ($\mu\text{mol } aa \text{ g}^{-1} \text{ DW}$)
aa_{cyt}	Cytosolic amino acid concentration ($\mu\text{mol } aa \text{ g}^{-1} \text{ DW}$)
$prot$	Protein concentration ($\mu\text{mol } N \text{ g}^{-1} \text{ DW}$)
$prot_{chlor}$	Chloroplast protein concentration ($\mu\text{mol } N \text{ g}^{-1} \text{ DW}$)
$prot_{cyt}$	Cytosolic protein concentration ($\mu\text{mol } N \text{ g}^{-1} \text{ DW}$)
$Ins. C$	Insoluble carbohydrate concentration ($\text{mg } C \text{ g}^{-1} \text{ DW}$)
$Sol. C$	Soluble carbohydrate concentration ($\text{mg } C \text{ g}^{-1} \text{ DW}$)
Flows	
F_1	Net ammonia uptake rate ($\mu\text{mol } NH_4^+ \text{ g}^{-1} \text{ DW h}^{-1}$)
F_2	Net amino acid synthesis ($\mu\text{mol } aa \text{ g}^{-1} \text{ DW h}^{-1}$)
F_3	Net protein synthesis ($\mu\text{mol } N \text{ g}^{-1} \text{ DW h}^{-1}$)
F_{3chlor}	Net protein synthesis in chloroplast ($\mu\text{mol } N \text{ g}^{-1} \text{ DW h}^{-1}$)
F_{3cyt}	Net protein synthesis in cytosol ($\mu\text{mol } N \text{ g}^{-1} \text{ DW h}^{-1}$)
DT	Diffusive aa transport ($\mu\text{mol } aa \text{ g}^{-1} \text{ DW h}^{-1}$)
ST	Stimulated aa transport ($\mu\text{mol } aa \text{ g}^{-1} \text{ DW h}^{-1}$)
$Trans.$	Net aa transport ($DT+ST$) ($\mu\text{mol } aa \text{ g}^{-1} \text{ DW h}^{-1}$)
G_1	Net photosynthesis rate ($\text{mg } C \text{ g}^{-1} \text{ DW h}^{-1}$)
G_2	Net rate of insoluble carbohydrate mobilization ($\text{mg } C \text{ g}^{-1} \text{ DW h}^{-1}$)
G_3	Whole C requirement to support N assimilation ($\text{mg } C \text{ g}^{-1} \text{ DW h}^{-1}$) (fixed stoichiometry of 6 mol C per mol assimilated N)
$(G_3 - G_1)$	Net C mobilization/accumulation, considering that G_1 is directed towards N assimilation, or stored in the case of N depletion ($\text{mg } C \text{ g}^{-1} \text{ DW h}^{-1}$)
Parameters	
F_{1max}	Maximum net ammonia uptake rate ($\mu\text{mol } NH_4^+ \text{ g}^{-1} \text{ DW h}^{-1}$)
K_{sF_1}	Semisaturation constant for ammonia uptake ($\mu\text{mol } NH_4^+ \text{ g}^{-1} \text{ DW}$)
$F_{3cytmax}$	Maximum rate of protein synthesis in cytosol ($\mu\text{mol } N \text{ g}^{-1} \text{ DW h}^{-1}$)
$K_{saa_{cyt}}$	Semisaturation constant of protein synthesis in cytosol ($\mu\text{mol } aa_{cyt} \text{ g}^{-1} \text{ DW}$)
d	Diffusion constant for aa transport (h^{-1})
ST_{max}	Maximum rate of stimulated aa transport ($\mu\text{mol } aa \text{ g}^{-1} \text{ DW h}^{-1}$)
K_{sST}	Semisaturation constant for stimulated aa transport ($\mu\text{mol } aa \text{ g}^{-1} \text{ DW h}^{-1}$)
nH	Hill exponent
G_{2max}	Maximum rate of insoluble carbohydrate mobilization ($\text{mg } C \text{ g}^{-1} \text{ DW h}^{-1}$)
CP_{G_2}	External NH_4^+ compensation point for insoluble carbohydrate mobilization ($\mu\text{mol } NH_4^+ \text{ g}^{-1} \text{ DW}$)
K_{sG_2}	Semisaturation constant for insoluble carbohydrate mobilization ($\mu\text{mol } NH_4^+ \text{ g}^{-1} \text{ DW}$)

From this point, we simulated the processes of aa and protein synthesis, taking into account the subcellular compartmentalization between chloroplast and cytosol and imposing a number of theoretical assumptions to be checked. The aa concentration in the chloroplast (aa_{chlor}) will be affected by the rate of aa synthesis (F_2), which takes place primarily in the chloroplast (Fisher & Klein 1988), by the aa transport between chloroplast and cytosol ($Trans.$) and by the net rate of protein synthesis in chloroplast (F_{3chlor}):

$$\frac{d[aa_{chlor}]}{dt} = F_2 - Trans. - F_{3chlor} \quad (6)$$

The aa concentration in the cytosol (aa_{cyt}) will be affected by the rate of aa transport ($Trans.$), and by the rate of protein synthesis in cytosol (F_{3cyt}):

$$\frac{d[aa_{cyt}]}{dt} = Trans. - F_{3cyt} \quad (7)$$

The variation of the chloroplast proteins will depend on the net rate of protein synthesis in this organelle:

$$\frac{d[prot_{chlor}]}{dt} = F_{3chlor} \quad (8)$$

and, in the same way, cytosolic proteins will be affected by the net rate of protein synthesis in the cytosol:

$$\frac{d[prot_{cyt}]}{dt} = F_{3cyt} \quad (9)$$

Nitrogen flows. The time course of the different internal N variables will depend on the flows established among them. In this study, a variable flow of N was maintained, as external NH_4^+ concentration did not remain constant with time. The first rate to be considered is the uptake of external NH_4^+ (F_1), which is fitted to a typical saturation kinetic:

$$F_1 = F_{1max} \frac{[NH_4^+ Ext.]}{[NH_4^+ Ext.] + K_{sF_1}} \quad (10)$$

External NH_4^+ concentration is expressed as $\mu\text{mol } NH_4^+ \text{ g}^{-1} \text{ DW}$ (scaled to culture density; i.e. 200 $\mu\text{M } NH_4^+$ represents 454.5 $\mu\text{mol } NH_4^+ \text{ g}^{-1} \text{ DW}$). The maximum net uptake rate (F_{1max})

= 75 $\mu\text{mol NH}_4^+ \text{ g}^{-1} \text{ DW h}^{-1}$) and the semisaturation constant ($K_{sF_1} = 118 \mu\text{mol NH}_4^+ \text{ g}^{-1} \text{ DW}$) were taken from Vergara et al. (1995).

The net rate of aa synthesis, also estimated from the previous experimental approach (Vergara et al. 1995), is a linear function of the rate of uptake of external NH_4^+ in the range assayed:

$$F_2 = -0.7 + 0.97 F_1 \quad (11)$$

In the same way, the net rate of protein synthesis is a linear function of the rate of aa synthesis:

$$F_3 = 12.6 + 0.60 F_2 \quad (12)$$

Amino acid transport. In a first approach, there will be a diffusive transport (DT) according to the concentration gradient of aa between the chloroplast and the cytosol:

$$DT = d([aa_{\text{chlor}}] - [aa_{\text{cyt}}]) \quad (13)$$

The aa flow is governed by a concentration gradient. The magnitude of the process will depend on the rate of the diffusion constant, 'd'. The default value was set at 0.05 h^{-1} . As it will be seen below, the alteration of this parameter had little effect on the end response of the simulations. As this diffusive process is dependent on a concentration gradient, this approach is valid whenever chloroplast and cytosolic volumes are similar. Despite some variability, several data in red algae indicate that chloroplast volume is about 50% of the protoplasm volume (Cunningham et al. 1992).

According to this approach, aa transport is a passive process dependent on a concentration gradient, and it is not modulated by the activity of aa synthesis. The process has been modified with the introduction of a term of stimulated transport depending on the need of C skeletons for inorganic N assimilation into aa. Chloroplasts display a differential permeability to several compounds, with the internal chloroplast membrane being the limiting step (Heldt 1976). Dicarboxylate transport is an active process (Lehner & Heldt 1978). Although dicarboxylate shuttles do not have an exact stoichiometry as with other shuttle systems (Flügge & Heldt 1991), an elevated entrance of organic acids in the chloroplast will cause a net export of aa from the chloroplast. We have considered aa transport as a sigmoid function of the rate of aa synthesis in chloroplast:

$$ST = ST_{\text{max}} \frac{F_2^{nH}}{F_2^{nH} + K_{sST}^{nH}} \quad (14)$$

The maximum rate of stimulated transport (ST_{max}) was set at 10 $\mu\text{mol aa g}^{-1} \text{ DW h}^{-1}$, which is on the same order of magnitude as the values reported *in vitro* in spinach chloroplasts (Lehner & Heldt 1978). The semisaturation constant (K_{sST}) is set at half of the maximum

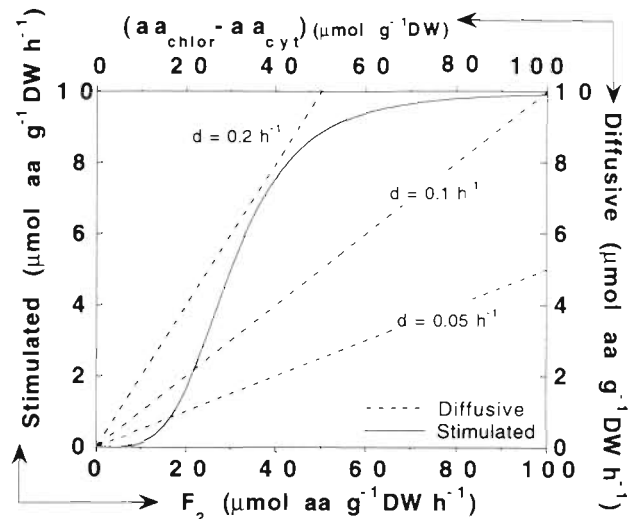


Fig. 2. Simulated functions of aa transport between chloroplast and cytosol. Diffusive component as a function of the difference of aa concentration between chloroplast and cytosol ($aa_{\text{chlor}} - aa_{\text{cyt}}$), the direction depending on the concentration gradient. Different values for the diffusion constant d are shown. Stimulated transport, as a function of the rate of aa synthesis (F_2), fitted to a sigmoidal curve (maximum rate of aa synthesis observed experimentally was about 60 $\mu\text{mol aa g}^{-1} \text{ DW h}^{-1}$, Vergara et al. (1995)

rate of aa synthesis (30 $\mu\text{mol aa g}^{-1} \text{ DW h}^{-1}$), and the exponent nH at 4.

The magnitude of aa transport by a diffusive process (a linear function, the direction depending on the gradient established) and by stimulated transport is plotted in Fig. 2. The resulting transport is the net balance between diffusive and stimulated transport, which can act in either the same or reverse direction (Eqs. 13 & 14):

$$Trans. = d([aa_{\text{chlor}}] - [aa_{\text{cyt}}]) + ST_{\text{max}} \frac{F_2^{nH}}{F_2^{nH} + K_{sST}^{nH}} \quad (15)$$

Protein synthesis. The rate of protein synthesis in cytosol is assumed to be a saturation function with respect to the aa concentration in this compartment:

$$F_{3\text{cyt}} = F_{3\text{cytmax}} \frac{[aa_{\text{cyt}}]}{[aa_{\text{cyt}}] + K_{saa\text{cyt}}} \quad (16)$$

The maximum rate chosen ($F_{3\text{cytmax}} = 40 \mu\text{mol g}^{-1} \text{ DW h}^{-1}$) is $\frac{2}{3}$ of the maximum rate of protein synthesis observed experimentally, and the semisaturation constant ($K_{saa\text{cyt}} = 120 \mu\text{mol N g}^{-1} \text{ DW}$) is half of the initial aa concentration (that is, the initial concentration of aa in the cytosol in the default simulation of 1:1).

The rate of protein synthesis in the chloroplast is the difference between overall protein synthesis (estimated from experimental results, Vergara et al. 1995) and the rate of protein synthesis in cytosol (Eq. 12 – Eq. 16):

$$F_{3\text{chlor}} = (12.6 + 0.6F_2) - F_{3\text{cyt}} \quad (17)$$

The simulations started with the same initial concentrations as those in our previous study (Vergara et al. 1995). To simulate the response at the subcellular level (cytosol and chloroplast) we must define a number of initial conditions. Simulations were carried out at different initial proportions of aa for chloroplast and cytosol. From the initial aa concentration (240 $\mu\text{mol aa g}^{-1}\text{DW}$), we used different ratios of aa for chloroplast and cytosol: 1:1 (default value; 120 $\mu\text{mol aa g}^{-1}\text{DW}$ in both compartments), 2cyt:1chlor, and 1cyt:2chlor. The diffusion constant d was simulated at rates of 0.05 (default value), 0.1 and 0.2 h^{-1} . With respect to the proteins, it is of interest to know the selective variation of the flow of N towards cytosolic or chloroplast proteins. Assuming that proteins have 14% content of N, there were 255 $\mu\text{mol N g}^{-1}\text{DW}$ in the initial state, 55 $\mu\text{mol N g}^{-1}\text{DW}$ of which were associated with phycobiliproteins (PBP) (Vergara et al. 1995). In the simulations, we established the following conditions (g^{-1}DW): 100 $\mu\text{mol N}$ in chloroplast proteins: 55 $\mu\text{mol N}$ in PBP and 45 $\mu\text{mol N}$ in Rubisco plus other soluble chloroplast proteins. Of the remaining proteins, 155 $\mu\text{mol N}$ are thus located initially in cytosolic soluble proteins. These concentrations represent an initial ratio of phycobiliproteins:soluble proteins (PBP:SP) similar to experimental data (21.5%), and an initial proportion of chloroplast proteins:soluble proteins to be 39.2%.

Difference equations of C metabolism. In relation to C variables, the variation of the concentration of insoluble carbohydrates is defined by a rate of mobilization or accumulation of C, G_2

$$\frac{d[\text{Ins.C}]}{dt} = -G_2 \quad (18)$$

The control of the concentration of soluble carbohydrates is shared among several flows. It will depend on a photosynthetic entrance of C (G_1), an input/output by mobilization/accumulation of insoluble carbohydrates (G_2), and an output of C to be cycled in a respiratory pathway (G_3):

$$\frac{d[\text{Sol.C}]}{dt} = G_1 + G_2 - G_3 \quad (19)$$

Carbon flow. The rate G_1 represents the C entrance by photosynthesis. Two values were assayed. We assume a value of 1 $\text{mg C g}^{-1}\text{DW h}^{-1}$ at a subsaturating irradiance of 80 $\mu\text{mol m}^{-2}\text{s}^{-1}$ (Vergara et al. 1995), and of 2 $\text{mg C g}^{-1}\text{DW h}^{-1}$ at saturating irradiances, close values to those for other *Gracilaria* species (Beer & Levy 1983, García-Sánchez et al. 1993).

The rate of C mobilization from reserve structures (G_2) was fitted to a saturation curve with respect to

external NH_4^+ availability. When NH_4^+ becomes limiting, there is a net C accumulation in reserve structures ($G_2 < 0$) while C is mobilized in response to a transient N assimilation ($G_2 > 0$):

$$G_2 = G_{2\text{max}} \frac{[\text{NH}_4^+ \text{Ext.}] - CP_{G_2}}{[\text{NH}_4^+ \text{Ext.}] + K_{sG_2}} \quad (20)$$

The values chosen for the parameters (maximum rate of C mobilization, $G_{2\text{max}} = 2.4 \text{ mg C g}^{-1}\text{DW h}^{-1}$; compensation point for NH_4^+ , $CP_{G_2} = 45 \mu\text{mol NH}_4^+ \text{ g}^{-1}\text{DW}$; and the semisaturation constant, $K_{sG_2} = 170 \mu\text{mol NH}_4^+ \text{ g}^{-1}\text{DW}$) fit well with our experimental results. The variation of these parameters does not affect the overall mobilization of C, which is set by the requirement of C skeletons for N assimilation. It only affects the relative degree of mobilization of insoluble and soluble carbohydrates.

The rate of mobilization of carbon (G_3) was considered to be a function of the rate of aa synthesis (F_2). We assume the stoichiometry of 6 atoms of C per atom of N assimilated in aa (Elfiri & Turpin 1986). A relation deviating from this will imply an accumulation or drain of intermediary C metabolites (mainly from the tricarboxylic acid cycle in the mitochondrion):

$$\begin{aligned} \frac{6 \mu\text{mol C}}{\mu\text{mol N}} \times \frac{12 \text{ mg C}}{\text{mmol C}} \times \frac{1 \text{ mmol C}}{1000 \mu\text{mol C}} \\ = 0.072 \text{ mg C } \mu\text{mol}^{-1} \text{ N} \end{aligned} \quad (21)$$

Therefore,

$$G_3 = 0.072F_2 \quad (22)$$

G_3 is the whole C requirement to meet N assimilation. The difference ($G_3 - G_1$) is the net mobilization of C from the insoluble and soluble carbohydrate pools, considering that all the entrance of C by photosynthesis is directed towards aa synthesis during transient N assimilation, or accumulated in C reserves in the case of N depletion. This is a net balance, which is measurable from our experimental results regardless the data about the photosynthetic C supply. The initial concentrations of insoluble and soluble carbohydrates simulated were those observed in the experimental approach (Vergara et al. 1995).

RESULTS AND DISCUSSION

This model is intended to understand ecological phenomena such as transient N assimilation in red algae, which is of importance in a system where N is intermittently supplied, and its connection with cell C dynamics, as N assimilation is dependent on photosynthetic C metabolism. However, as pointed out by Scheffer et al. (1993), the versatility of a simulation

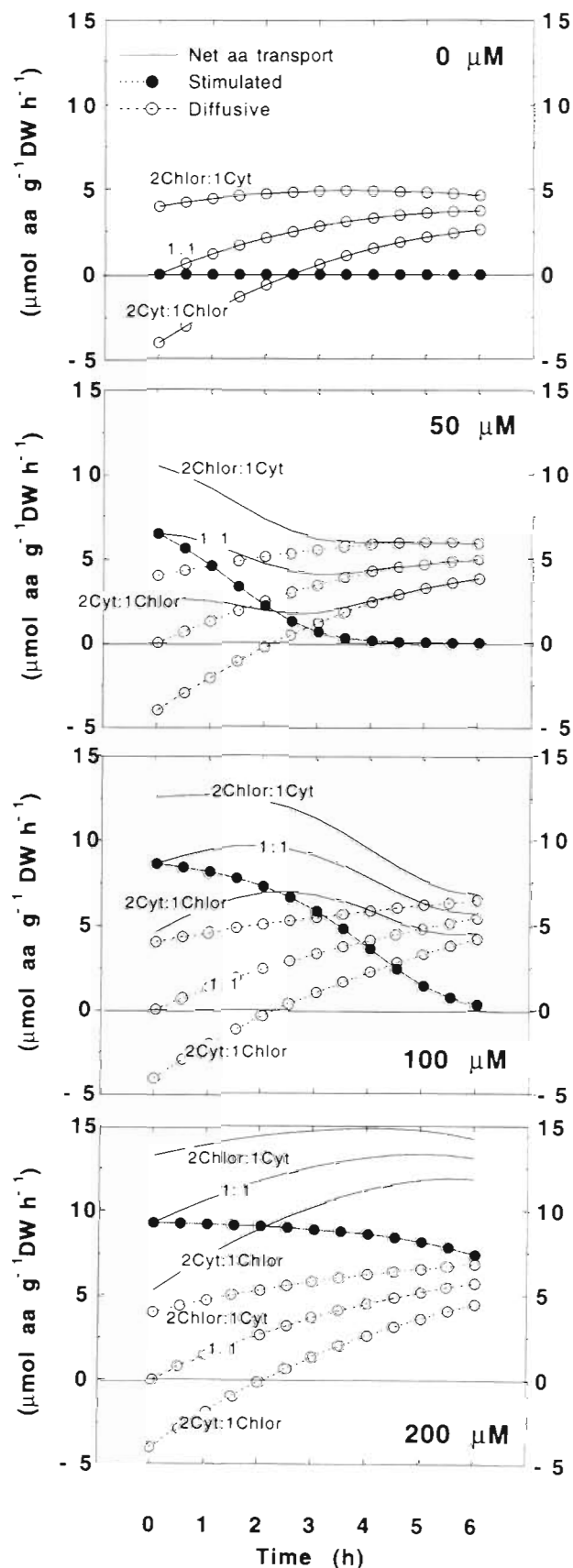
model allows us to project a large variety of different simulation experiments. A complete account of the potential behavior under different circumstances (external N availability, photosynthetic C entrance, internal concentration and changes in the allocation of N and C compounds, wide range of parameter settings) cannot be given. Therefore, the results presented here are compared with the experimental results that have been determined previously for the red alga *Gracilariopsis lemaneiformis* (Vergara et al. 1995).

Amino acid transport

As expected, intermediary N compounds (internal NH_4^+ and aa) showed a concentration that was similar to the experimental ones after 6 h (data not shown), since the rates of N flow were derived from the data obtained in the experimental approach. The time course of aa transport between chloroplast and cytosol at different initial NH_4^+ pulses is shown in Fig. 3. The aa transport is a net balance between a diffusive component, which depends on the difference of aa concentration between the 2 compartments, and a stimulated transport, which is a function of the rate of aa synthesis in the chloroplast. A default value of the diffusion constant of $d = 0.05 \text{ h}^{-1}$ was simulated. We assayed 3 distinct initial distributions of aa between chloroplast and cytosol (percentages 1cyt:1chlor, 1cyt:2chlor, and 2cyt:1chlor). Positive values represent a net outflow of aa from the chloroplast to the cytosol, and conversely, negative values represent a net inflow of aa into the chloroplast.

In the absence of an external source of N (no NH_4^+ added), active transport is considered null because of the lack of demand of organic acids, and aa transport is only driven by a diffusive process, which depends on the difference of concentration of aa between chloroplast and cytosol (Fig. 3). The larger the initial NH_4^+ pulse, the higher the activity of stimulated transport, this activity being close to the maximum rate (ST_{max}) after 100 and 200 μM NH_4^+ pulses, and decreasing with time as a consequence of the drop in aa synthesis,

Fig. 3. Time course of aa transport between the chloroplast and the cytosol at different initial NH_4^+ pulses (0 to 200 μM). Different initial aa allocations between chloroplast and cytosol were assayed (ratios 1:1, 1chlor:2cyt, and 2chlor:1cyt); the diffusion constant d was fixed at the default value (0.05 d^{-1}). The aa transport is a net balance between a diffusive and a stimulated component. Positive values represent a net outflow of aa from the chloroplast, and negative ones a net inflow into the chloroplast



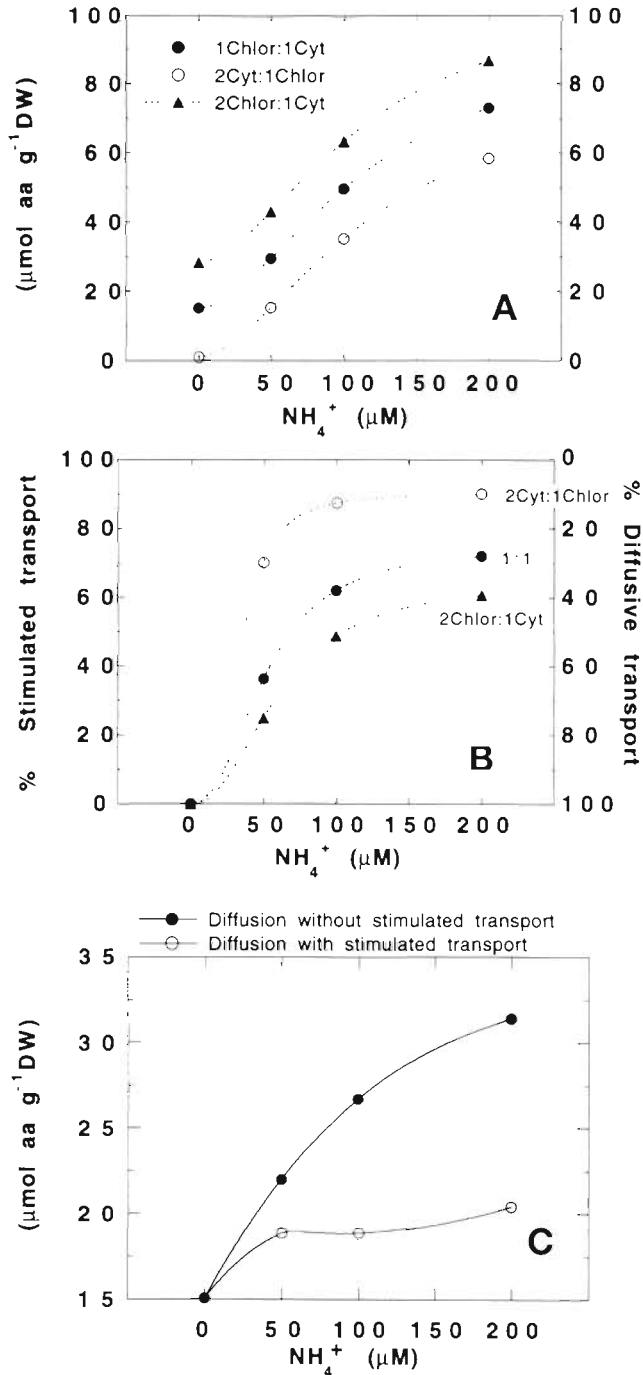


Fig. 4. (A) Integrated net aa transport from the chloroplast to the cytosol during the period of the experiment (6 h) at different initial NH_4^+ pulses, assaying a different initial aa allocation between chloroplast and cytosol (ratios 1:1, 1chlor:2cyt, and 2chlor:1cyt); the diffusion constant d was set at the default value (0.05 d^{-1}). The data represent integrates in time from Fig. 3. (B) Contributions of stimulated and diffusive transport in the net aa transport, as a function of initial NH_4^+ pulses and initial aa distribution. (C) Diffusive aa transport during the period of the experiment (6 h) as a function of initial NH_4^+ supply, either when a diffusive component was assayed alone or when there was a co-occurring stimulated aa transport

which in turn is caused by the drop of external NH_4^+ concentration.

The time course of diffusive transport is affected more by the initial distribution of aa inside and outside the chloroplast assayed than by the rate of aa synthesis (which is strongly influenced by external NH_4^+ availability). Stimulated transport is assumed not to be affected by the particular stoichiometry of aa in chloroplast and cytosol, as it depends on the net rate of aa synthesis in the chloroplast.

The process outlined above (Fig. 3) shows the time course of aa transport. The integration of the area under these curves represent the net transport of aa during the period of the experiment (6 h). The net aa transport displayed a sigmoidal curve with respect to external NH_4^+ supply. In addition, aa transport was greater as the initial aa concentration was higher in the chloroplast, as a consequence of an enhanced diffusive component (Fig. 4A). The relative contributions of the diffusive component and of the stimulated transport are shown in Fig. 4B. Diffusive transport was important when the initial NH_4^+ pulse was lower. This component was further enhanced as the initial aa levels were higher in chloroplast. However, the differences that we will find in protein synthesis assuming stimulated transport or a diffusive component alone are lower than those one might expect *a priori* (see Fig. 7, for instance). This is because stimulated aa transport reduces the aa concentration gradient between chloroplast and cytosol, and therefore, diffusive transport becomes less relevant when a stimulated transport is also assayed (Fig. 4C). As a result of the processes of aa transport and of the activities of aa and protein synthesis in chloroplast and cytosol (described below), the aa concentration tends to increase in the chloroplast (aa synthesis in the chloroplast) and to decrease in the cytosol, despite the net outflow of aa from the chloroplast (Fig. 5). For each pulse of external NH_4^+ , the initial aa distribution between chloroplast and cytosol has little effect on the end aa concentration in both compartments, as there was a tendency towards certain levels of equilibrium between chloroplast and cytosol (Fig. 5). The setting of this equilibrium is shared among the processes of diffusive transport, aa synthesis in chloroplast and the protein synthesis in both compartments. The diffusive component will become relevant when a high aa gradient is established, as a tendency to equalize the aa concentrations. The aa concentration in each compartment is also affected by the initial NH_4^+ pulse, which determines the magnitude of aa synthesis rate. When the aa synthesis rate is high, there is an accumulation of aa in the chloroplast, despite high rates of protein synthesis in chloroplast (described below), as well as high rates of net aa outflow towards the cytosol.

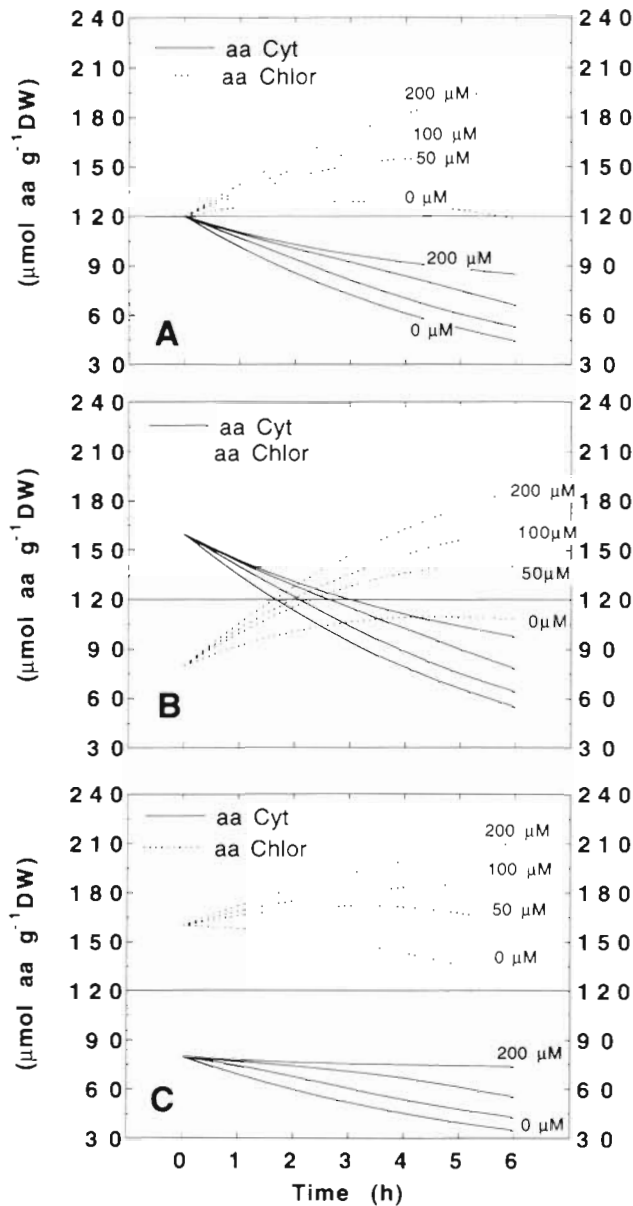


Fig. 5. Time course of aa concentration in the chloroplast (dashed lines) and the cytosol (solid lines) at different initial NH_4^+ pulses. (A) Initial distribution $120 \mu\text{mol aa g}^{-1} \text{DW}$ on each compartment; (B) $160 \mu\text{mol aa g}^{-1} \text{DW}$ in the cytosol and $80 \mu\text{mol aa g}^{-1} \text{DW}$ in the chloroplast; (C) $80 \mu\text{mol aa g}^{-1} \text{DW}$ in the cytosol and $160 \mu\text{mol aa g}^{-1} \text{DW}$ in the chloroplast. Default value used for $d = 0.05 \text{ h}^{-1}$.

Protein synthesis

Ultimately, the importance of having an approximate knowledge of the processes of aa transport relies on the fact that it will determine the rates of protein synthesis in cytosol and chloroplast, as aa transport interacts with the concentrations of aa in both compartments. The rate of protein synthesis, estimated from

the experimental results, is a linear function of the rate of aa synthesis for the range of NH_4^+ pulses and of time period assayed ($F_3 = 12.6 + 0.6 F_2$). This function indicates that some of the preexisting aa are used in protein synthesis during N limitation, while an excess of aa are synthesized when the pulse of NH_4^+ is high, which may saturate the rate of protein synthesis. The rate of protein synthesis in cytosol ($F_{3\text{cyt}}$) was set as a saturation function of the aa concentration in the cytosol, and the rate of protein synthesis in chloroplast ($F_{3\text{chlor}}$) as the difference between F_3 and $F_{3\text{cyt}}$. Thus, protein synthesis was not only affected by the assimilation of inorganic N into aa, but also by the aa transport between chloroplast and cytosol. The time course of the rate of protein synthesis in chloroplast and cytosol at different pulses of external NH_4^+ is shown in Fig. 6. Chloroplast protein synthesis was strongly influenced by the magnitude of NH_4^+ pulses, unlike cytosolic ones. In the absence of NH_4^+ supply, there was a net protein degradation in chloroplast ($F_3 < 0$), while protein synthesis in cytosol was maintained close to an optimum level. In contrast, protein synthesis in chloroplast was higher than that in cytosol in response to a $200 \mu\text{M}$ NH_4^+ pulse. Thus, in the short-term (hours), cytosolic protein synthesis is, unlike that for the chloroplast, rather independent of external NH_4^+ supply.

The relative importance of PBP within the soluble protein pool is indicated by the ratio PBP:SP (Vergara & Niell 1993, Vergara et al. 1995). If PBP changed in the same proportion as the other proteins, it would indicate a generalized and not a selective response of PBP to N starvation or N supply. The initial hypothesis to consider is that the PBP follow a more general response of chloroplast proteins to N availability. The PBP:SP ratios

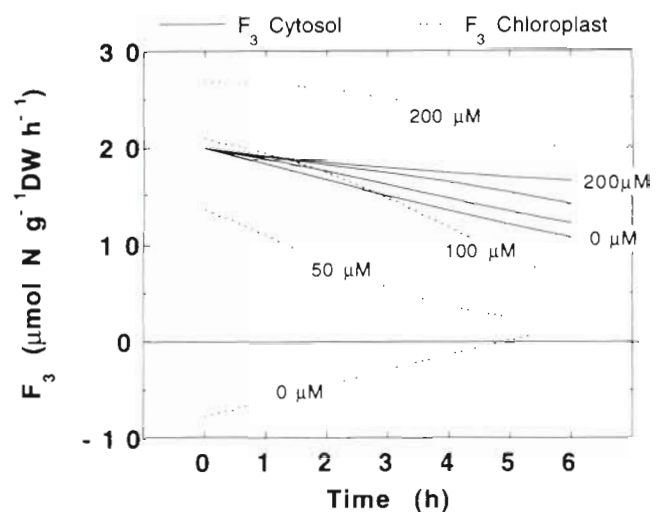


Fig. 6. Time course of net protein synthesis in the chloroplast and the cytosol at different initial NH_4^+ pulses, in the default simulations (diffusive and stimulated aa transport; $d = 0.05 \text{ h}^{-1}$; initial aa distribution between chloroplast and cytosol 1:1).

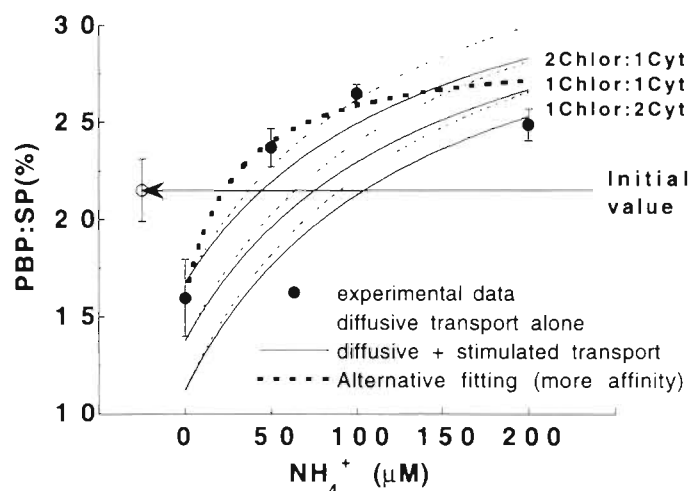


Fig. 7. Predicted values of the ratio PBP:SP and those observed experimentally in response to different NH_4^+ pulses after 6 h. Predicted ratios were assayed at 3 different initial ratios of aa in the chloroplast and the cytosol, assuming a diffusive component alone or coupled to a stimulated transport. The thick dashed line shows an alternative curve representing a N response with more affinity to N supply

derived from the model, assuming different kinds of aa transport, for different initial aa distributions between chloroplast and cytosol, together with the experimental data from Vergara et al. (1995) are depicted in Fig. 7. The ratio PBP:PS displayed a saturation curve with respect to external NH_4^+ availability. In optimal conditions, a maximum PBP content is expected to occur, constrained by a maximum density of phycobilisomes per thylakoid area, while SP concentration can further increase. It can eventually lead to a decline of the PBP:SP ratio. In contrast, during N limitation, the period of time over which algae were subjected to N starvation will determine the degree of mobilization of PBP. In our approach, PBP mobilization is studied in the short-term (hours), thus holding PBP concentration at physiological levels. In the long-term, a prolonged N starvation promotes an obvious bleaching of the red algae (Bird et al. 1982, Vergara et al. 1993). The response of chloroplast proteins to NH_4^+ availability will be influenced by the rate of aa synthesis in the chloroplast, the transport phenomena of aa between chloroplast and cytosol, and by the rates of protein synthesis in both compartments. An assay of a diffusive transport of aa alone, or coupled to a stimulated transport, revealed some variations of PBP:SP ratio which were lower than those promoted by the initial aa distribution between chloroplast and cytosol. In fact, differ-

ent rates of diffusive transport (d from 0.05 to 0.2 h^{-1}) modified the PBP:SP ratio less than a different initial aa ratio between chloroplast and cytosol or the assay of different kinds of transport (data not shown). The ratio was kept higher if the initial aa concentration was larger in the chloroplast (E_0 term, see Table 2). However, the affinity (estimated by the semisaturation constant) was affected neither by the initial aa distribution nor the assay of a diffusive compartment or when it is coupled to stimulated transport. The maximum PBP:SP ratio attained was slightly lowered by the application of a stimulated transport.

However, this is the result when a constant relation between PBP and plastid proteins is considered. Alternatively, experimental data could be also fitted to a saturation curve with a higher affinity to N supply (lower K_s). This fitted curve reached saturation at lower external NH_4^+ concentrations, and the maximum PBP:SP ratio was lower than those attained by the simulations (Table 2). As indicated in a previous study (Vergara et al. 1995), changes in the abundance of photosynthetic proteins are not proportional to N limitation (Falkowski et al. 1989), the rate of plastid protein synthesis being controlled at a translational level (Plumley & Schmidt 1989). PBP seems to follow a more general response of plastid proteins. Other chloroplast proteins such as Rubisco will also be affected by N availability in red algae (García-Sánchez et al. 1993), where both Rubisco subunits are chloroplast-encoded proteins (Valentin & Zetsche 1989). Thus, this hypothesis becomes relevant in these organisms, where 2 of the more abundant proteins are chloroplast encoded (PBP accounting for about 25% and Rubisco for about 10% of soluble proteins).

Table 2. Parameters of the ratio PBP:SP, as a saturation function of external NH_4^+ availability after 6 h, including different kinds of aa transport as well as different initial aa ratios between chloroplast and cytosol. Curves were fitted to a saturation curve plus an E_0 term (value of the PBP:SP ratio when external NH_4^+ is zero). K_s (semisaturation constant, $\mu\text{M NH}_4^+$). V_{max} (maximum variation of the PBP:SP ratio); Max (maximum PBP:SP ratio attained, $\text{Max} = E_0 + V_{\text{max}}$). Values for an alternative curve fitting of the experimental data are also shown

Parameter:	Diffusive aa transport				Diffusive plus stimulated aa transport			
	E_0	K_s	V_{max}	Max	E_0	K_s	V_{max}	Max
Initial aa ratio:								
2cyt:1chlor	11.2	133	25.5	36.7	11.2	134	23.5	34.7
1cyt:1chlor	13.8	134	24.0	37.8	13.8	135	21.6	35.4
1cyt:2chlor	16.7	135	22.2	38.9	16.7	136	19.5	36.2
Alternative curve fitting	15.9	30	12.9	28.8				

Mobilization of C during NH_4^+ assimilation

The second objective of the model was to assess the interaction between C and N metabolism during transient NH_4^+ assimilation in red algae. In normal conditions, C skeletons for aa synthesis are supplied by photosynthesis. However, when N assimilation exceeds photosynthetic C supply, carbohydrates become the main source of C for aa synthesis (Elfiri & Turpin 1987,

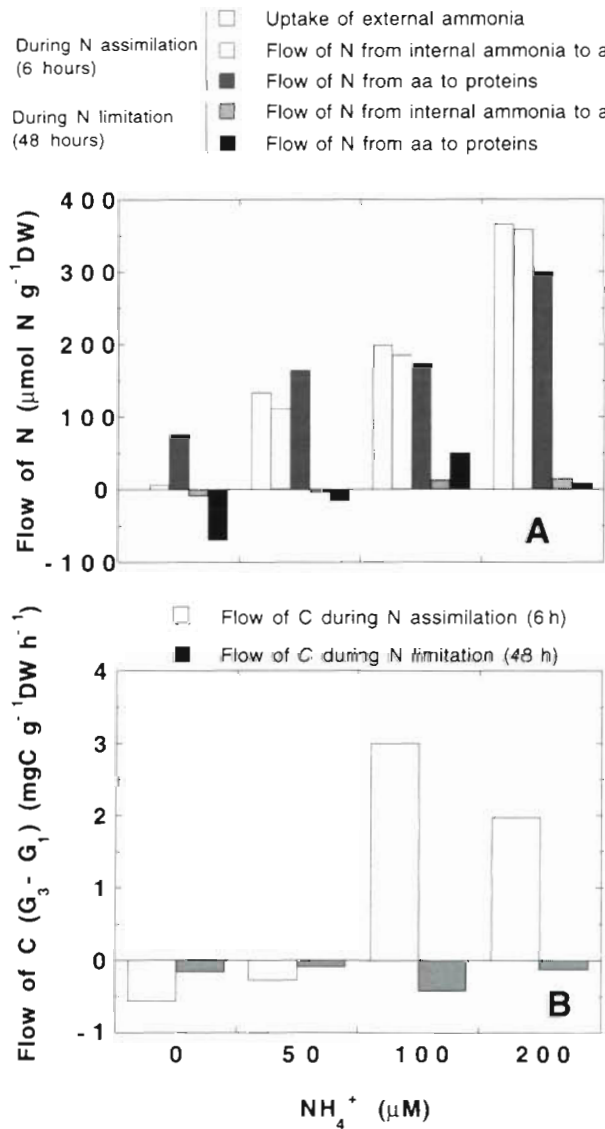


Fig. 8. (A) Net flow of N (NH_4^+ uptake, flow of N from internal NH_4^+ to aa and N from aa to proteins) ($\mu\text{mol N g}^{-1}\text{DW}$) during N assimilation following NH_4^+ pulses (6 h) and during subsequent N limitation (48 h). Data were not scaled to time to appreciate graphically the N flow during the period of N limitation. (B) Net flow of C from soluble and insoluble carbohydrates pools ($G_3 - G_1$) ($\text{mgC g}^{-1}\text{DW h}^{-1}$) during N assimilation following NH_4^+ pulses (6 h) and during subsequent N limitation (48 h). Data from Vergara et al. (1995)

Plumley & Schmidt 1989). Independent of the source of C (photosynthetic C or from reserve compounds) N assimilation enhances the C flow through respiratory pathways (Turpin et al. 1988). In a previous study, both soluble and insoluble carbohydrate concentrations

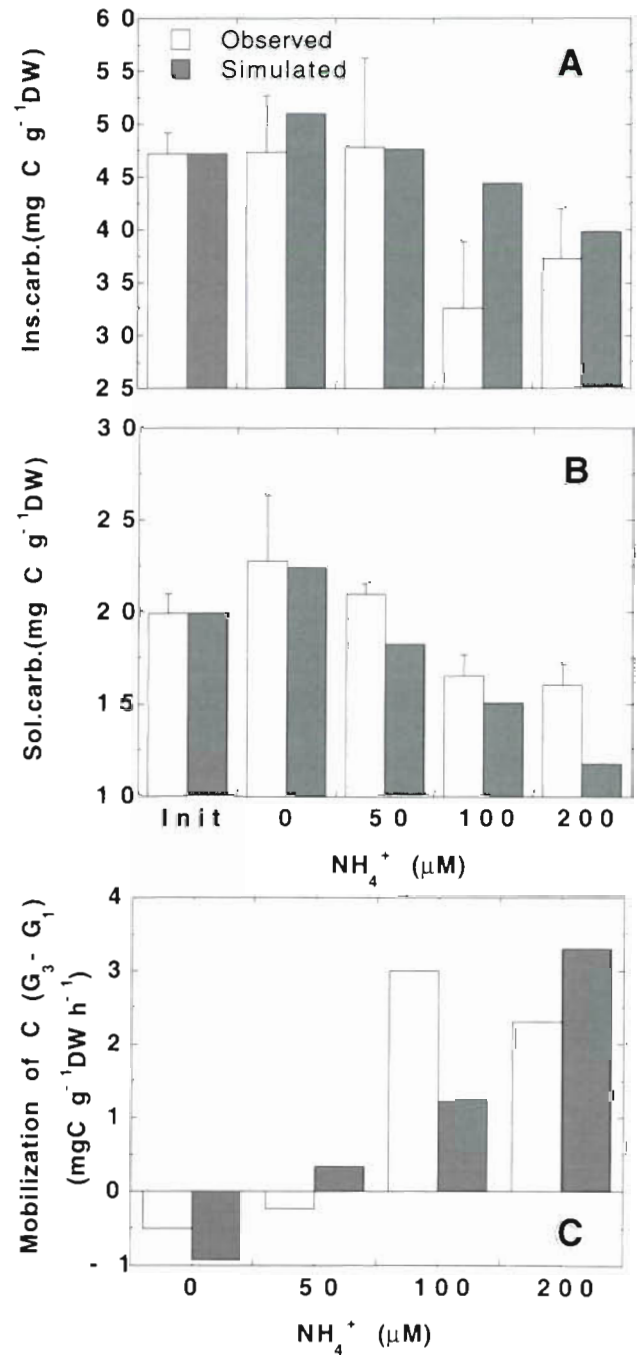


Fig. 9. Predicted and experimentally observed concentrations of (A) insoluble and (B) soluble carbohydrates in response to different NH_4^+ pulses after 6 h. (C) Predicted and observed rates of C mobilization ($G_3 - G_1 > 0$) or accumulation ($G_3 - G_1 < 0$) after 6 h in response to different NH_4^+ pulses

decreased in response to transient NH_4^+ assimilation in *Gracilariopsis lemaneiformis* (Vergara et al. 1995). In Fig. 8, the flow of N (NH_4^+ uptake, N flow from internal NH_4^+ to aa and N flow from aa to proteins during N assimilation (6 h) and subsequent N limitation (48 h) in parallel with the flow of C from carbohydrates (net mobilization rate, $G_3 - G_1$) are shown. Cell C was mobilized from carbohydrates in response to active NH_4^+ assimilation (100 and 200 μM NH_4^+ pulses). Conversely, carbohydrates were accumulated during N limitation (no NH_4^+ supply). Subsequently, in N limiting conditions, concomitant with a drastic reduction of N assimilation into aa, C mobilization from carbohydrates was restricted. There was an accumulation of carbohydrates on the same order of magnitude as in the control treatment without N supply, which may correspond to the photosynthetic C entrance (G_1).

The question is how to approximate the stoichiometry of C mobilization in response to N assimilation. Theoretically, 6 atoms of C (2 molecules C_3) are supposed to be necessary to assimilate 1 molecule of inorganic N into aa (Elfiri & Turpin 1986). Simulations were done with this constraint, considering the previously obtained experimental data and assuming a photosynthetic C fixation of $1 \text{ mg C g}^{-1} \text{ DW h}^{-1}$. The end concentrations of soluble and insoluble carbohydrates after 6 h, compared to the experimental data, are depicted in Fig. 9. Both data sets showed the same trend; carbohydrate content decreased following NH_4^+ addition. As a consequence, the C mobilization from carbohydrates occurred in response to an active N assimilation, while it was restricted during N limitation. The predicted rates of C mobilization showed the same trend as the observed data (Fig. 9C). Inserting this result into a more general model of interaction, there was a C mobilization when a high demand of C skeletons occurred, while C was accumulated in carbohydrates when N assimilation was impaired (Fig. 10). Thus, the stoichiometry of N assimilation (6 mol C per N mol) is essential in determining the cell C dynamics. Any deviation from this stoichiometry would result in an accumulation or a drain of intermediary C compounds, mainly from the tri-carboxylic acid cycle.

A variation in the proportion of insoluble carbohydrates within the cell C in response to transient N assimilation is expected (Vergara et al. 1995). This ratio, an indicator of C partitioning between C reserve structures and or-

ganic N compounds, is also affected by growth irradiance. In another agarophyte red alga, *Gelidium sesquipedale*, the ratio insoluble carbohydrates:total cell carbon increased when thalli were cultured at an irradiance of $100 \mu\text{mol m}^{-2} \text{ s}^{-1}$, while it decreased when algae were cultured at $40 \mu\text{mol m}^{-2} \text{ s}^{-1}$, despite a similar N supply (Carmona et al. 1996). Therefore, it could be hypothesized that at higher, saturating irradiances, the net C mobilization will be lower, despite a similar demand for C skeletons. The model was also simulated considering a greater C input from photosynthesis, causing a lower net C mobilization than at subsaturating irradiances (data not shown). The effects of N assimilation on C pools will be alleviated at light saturation.

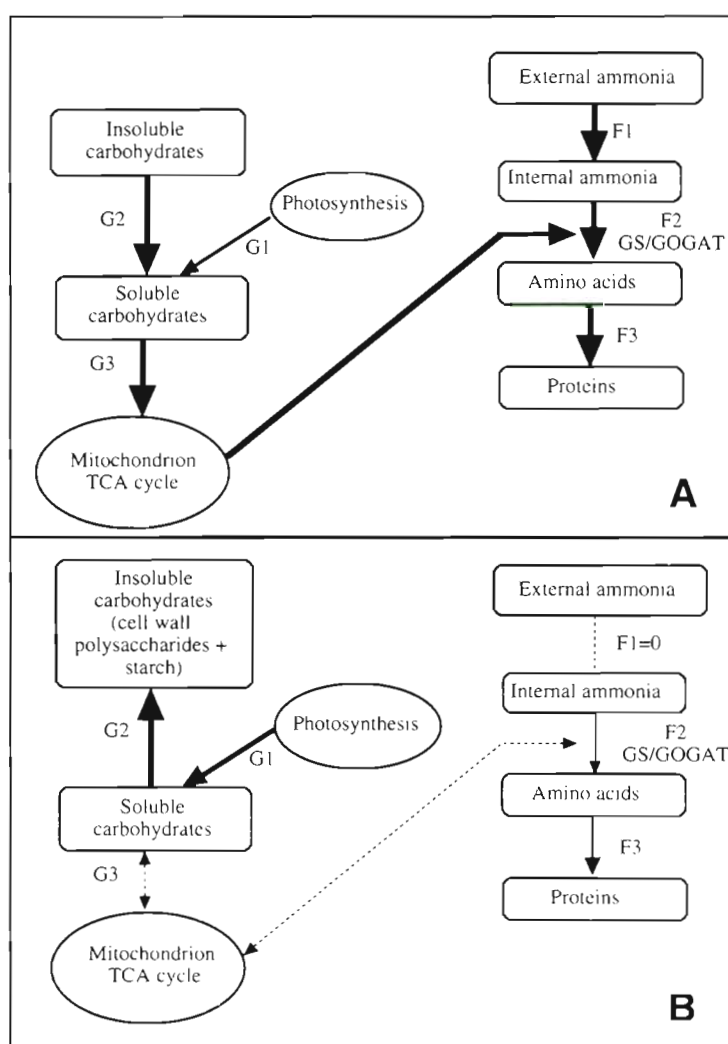


Fig. 10. Diagrammatic representation of the C flow during (A) transient N assimilation and (B) N limitation. In (A), photosynthetic C supply is not sufficient to maintain N assimilation into aa and proteins, and carbohydrates become the main C source, especially at subsaturating irradiances. In (B), photosynthetically fixed C is directed towards C reserve pools. The thickness of the arrows represents qualitatively the intensity of the flows

CONCLUSIONS

Here we present a simple dynamic model of transient N assimilation and subsequent C mobilization in a marine red alga at the subcellular level. The model predictions are in good agreement with the experimental data, indicating that some of the constraints imposed (the differential protein synthesis in chloroplast as a result of a translational control of protein synthesis, the close stoichiometry of C mobilization in response to N assimilation) are ecophysiologicaly relevant. The sensitivity of the model to the parameter settings indicates that it has a high robustness (Jørgensen 1986). Great changes in the initial balance of aa between chloroplast and cytosol, different parameter settings for the diffusion constant d , or even assuming aa transport promoted by 2 forces or a diffusive component alone caused minor changes in the end results of the simulations (see, for instance, the ratio PBP:SP; Fig. 7) in comparison with the variation of the external forcing function, in our case, the magnitude of the external NH_4^+ pulse. Some difficulties arise when the parameters, in some cases selected arbitrarily, cause a great change in the response of the system. With respect to C mobilization, the fixed stoichiometry of 6 C molecules per N molecule assimilated seems to be determinant in C partitioning between carbohydrates and organic N compounds, effects being especially noteworthy at subsaturating irradiance levels.

While we have made comparisons of the model's projections to experimental data for 1 species, it should be pointed out that the overall pattern of C and N allocation in *Gracilariopsis lemaneiformis* must be similar for a number of red algal species, such as *Gracilaria tikvahiae*, *Corallina elongata* and *Gelidium sesquipedale* (Bird et al. 1982, Vergara & Niell 1993, Vergara et al. 1993). While there are certain species-specific differences, for instance external NH_4^+ uptake rates, or cell C compartmentalization in non-agarophyte species, the similarities in C and N allocation patterns between these species suggest that this model may be a good initial approximation that can be applied to a large number of red algae. Experimental results from other rhodophyte species can serve to further test the robustness of the model.

However, it must be stressed that many of the limitations in our dynamic model can be only redressed by a focused experimental approach, as Geider et al. (1996) stated after developing a dynamic model of phytoplankton photoadaptation. The model can also be refined by including other processes not surveyed here (proteins synthesized in the cytosol and transported into the chloroplast, net leakage of soluble compounds from the cell, etc.). In addition, the model assumes instantaneous responses. Some simulations were done

assuming a time lag period; however, the end results were similar to those obtained in the present study (data not shown). Oscillations were only recorded when the time lag period was on the order of hours, a period of time close to the length of the simulation experiment. Despite these limitations, the model confers basic insights into the mechanisms of C-N interaction in marine red algae, linking metabolic mechanisms and subcellular compartmentalization to the ecophysiology of red macroalgae.

Acknowledgements. This research has been supported by the project of the CICYT (AMB93-1211) from the Ministerio de Educación y Ciencia (Spain).

LITERATURE CITED

- Beer S, Levy I (1983) Effects of photon fluence rate and light spectrum composition on growth, photosynthesis and pigment relations in *Gracilaria* sp. *J Phycol* 19:516–522
- Bird KT, Habig C, De Busk T (1982) Nitrogen allocation and storage patterns in *Gracilaria tikvahiae* (Rhodophyta). *J Phycol* 18:344–348
- Carmona R, Vergara JJ, Pérez-Lloréns JL, Figueroa FL, Niell FX (1996) Photosynthetic acclimation and biochemical responses of *Gelidium sesquipedale* cultured in chemostats under different qualities of light. *Mar Biol* 127:25–34
- Cunningham FX Jr, Vonshak A, Gantt E (1992) Photoacclimation in the red alga *Porphyridium cruentum*. *Plant Physiol* 100:1142–1149
- Elfiri IR, Turpin DH (1986) Nitrate and ammonium induced photosynthetic suppression in N-limited *Selenastrum minutum*. *Plant Physiol* 81:273–279
- Elfiri IR, Turpin DH (1987) The path of carbon flow during NO_3^- induced photosynthetic suppression in N-limited *Selenastrum minutum*. *Plant Physiol* 83:97–104
- Falkowski PG, Dubinsky Z, Wyman K (1985) Growth-irradiance relationship in phytoplankton. *Limnol Oceanogr* 30:311–321
- Falkowski PG, Sukenik A, Herzig R (1989) Nitrogen limitation in *Isochrysis galbana* (Haptophyceae). II. Relative abundance of chloroplast proteins. *J Phycol* 25:471–478
- Fisher P, Klein U (1988) Localization of nitrogen-assimilating enzymes in the chloroplast of *Chlamydomonas reinhardtii*. *Plant Physiol* 88:947–952
- Flügge UI, Heldt HW (1991) Metabolite translocators of the chloroplast envelope. *Annu Rev Plant Physiol Plant Mol Biol* 42:129–144
- García-Sánchez MJ, Fernández JA, Niell FX (1993) Biochemical and physiological responses of *Gracilaria tenuistipitata* under two different nitrogen treatments. *Physiol Plant* 86:631–637
- Geider RJ, MacIntyre HL, Kana TM (1996) A dynamic model of photoadaptation in phytoplankton. *Limnol Oceanogr* 41:1–15
- Heldt HW (1976) Metabolite carriers of chloroplast. In: Stocking CR, Heber U (eds) Transport in plants. Intracellular interactions and transport processes. Encyclopedia of plant physiology. Vol. 3. Springer-Verlag, Berlin, p 137–143
- Jeffries C (1988) Mathematical modelling in ecology. Birkhäuser, Boston
- Jørgensen E (1986) Fundamentals of ecological modelling. Elsevier, Amsterdam

- Kiefer DA, Mitchell BG (1983) A simple, steady-state description of phytoplankton growth based on absorption cross section and quantum efficiency. *Limnol Oceanogr* 28: 770–776
- Kremer JN, Nixon SW (1978) A coastal marine ecosystem. Simulation and analysis. Springer-Verlag, New York
- Laws EA, Chalup MS (1990) A microalgal growth model. *Limnol Oceanogr* 35:597–608
- Lehner K, Heldt HW (1978) Dicarboxylate transport across the inner membrane of the chloroplast envelope. *Biochim Biophys Acta* 501:531–544
- Mooney HA (ed) (1991) Responses of plants to multiple stress. Academic Press, New York
- Plumley FG, Schmidt GW (1989) Nitrogen-dependent regulation of photosynthetic gene expression. *Proc Natl Acad Sci USA* 86:2678–2682
- Scheffer M, Bakema AH, Wolterboer FG (1993) MEGA-PLANT: a simulation model of the dynamics of submerged plants. *Aquat Bot* 45:345–356
- Turpin DH, Elfiri IR, Birch DG, Weger HG, Holmes JJ (1988) Interactions between photosynthesis, respiration and nitrogen assimilation in microalgae. *Can J Bot* 66:2083–2097
- Valentin K, Zetsche K (1989) The genes of both subunits of ribulose-1,5-bisphosphate carboxylase constitute an operon on the plastome of a red alga. *Curr Gen* 16: 203–209
- Vergara JJ, Bird KT, Niell FX (1995) Nitrogen assimilation following NH_4^+ pulses in the red alga *Gracilariopsis lemaneiformis*. Effect on C metabolism. *Mar Ecol Prog Ser* 122: 253–263
- Vergara JJ, Niell FX (1993) Effects of nitrate availability and irradiance on internal nitrogen constituents in *Corallina elongata* (Rhodophyta). *J Phycol* 29:285–293
- Vergara JJ, Niell FX, Torres M (1993) Culture of *Gelidium sesquipedale* (Clem.) Born. et Thur. in a chemostat system. Biomass production and metabolic responses affected by N flow. *J Appl Phycol* 5:405–415
- Wiegert RG (1979) Population models: experimental tools for the analysis of ecosystems. In: Horn DJ, Mitchell RD, Stairs GR (eds) *Analysis of ecological systems*. Ohio Univ Press, Columbus, p 233–280
- Wulff F, Field JG, Mann KH (1989) Network analysis in marine ecology. Methods and applications. *Coastal and Estuarine Studies*, Vol. 32. Springer-Verlag, Berlin

This article was submitted to the editor

Manuscript first received: October 25, 1996

Revised version accepted: January 16, 1997